

Practical approaches for design of pile groups and piled rafts

Mark F, Randolph⁽¹⁾ and Oliver Reul⁽²⁾

⁽¹⁾ University of Western Australia, Australia <mark.randolph@uwa.edu.au>

⁽²⁾ Universität Kassel, Germany <o.reul@uni-kassel.de >

ABSTRACT. The last two decades have seen significant advances in understanding, analysis and design approaches for pile groups and piled rafts. These advances have been helped in no small measure by the accessibility and relatively low computational cost of full three-dimensional finite element analysis of pile group response, including increasingly sophisticated soil modelling. From a practical viewpoint, however, much simpler approaches are used routinely in design, at least for initial sizing and assessment of piled foundation response. This paper builds on recent contributions that have presented simple lumped models for the non-linear response of individual piles and pile groups, and the associated raft-soil interaction. The focus is on two main aspects: quantification of the role of non-linear response of individual piles in the load distribution among piles in a group and the overall group response; and the coupling of raft stiffness and pile group response in order to assess differential settlements and load distribution among the piles. Extension of existing software to incorporate non-linear pile response, and iterative linking with raft foundation analysis, are presented. The paper includes comparisons with rigorous numerical analysis and also with several case studies from the field.

1. INTRODUCTION

The purpose of foundation piles is to transmit loads from a superstructure to deep strata, which are generally stiffer and of higher strength than those near the ground surface. Generally the cap or basement slab above the piles will be cast directly on the ground and may contribute by transferring some of the superstructure loads directly to the soil, rather than via the piles, hence the term ‘piled raft’. From an analysis perspective, piles might be represented by (non-linear) springs attached to columns or a basement slab (the ‘raft’), with separate springs representing the axial and lateral response of the pile. Complexity arises, however, because of interactions between piles within a group, so that the springs are not independent. The interactions mainly affect their stiffness at operational loads, although overlapping of kinematic failure modes may also affect the limiting capacity, particularly for the horizontal response. This has led to increasingly sophisticated analysis techniques, in particular to quantify interaction coefficients between piles, starting from the basis of elastic soil response, but also allowing for local non-linearity whereby individual piles become increasingly decoupled from the rest of the pile group as they progress towards failure. For vertical loading, pile group capacity is generally very close to the sum of the individual pile capacities. However, under horizontal loading, potential reduction in the horizontal capacity of trailing piles within a group, a so-called ‘shadowing effect’, may also be incorporated.

Perhaps the most sophisticated analysis and design software for pile groups is REPUTE (Geocentrix 2017), which is based on the calculation algorithm PGROUPn (Basile 2003). As for much pile group analysis software, the underlying approach is the boundary element method (BEM) that emanates from the early pioneering work of Poulos (1968, 1989), and Butterfield and Banerjee (1971). Compared with the finite element method, the BEM has the virtue that only the

surface of each pile needs to be discretized into elements, rather than the full soil domain. Mindlin's (1936) solution is used to obtain a fully populated interaction matrix between all pile elements. Although strictly applicable only to soil domains where the modulus is homogeneous, an approximate approach of taking the average soil modulus between the two elements in question has been found to provide sufficient accuracy (Poulos 1979). BEM-based software for pile group analysis includes a series of tools such as DEFPIG and CLAP developed by Poulos.

Non-linearity may be handled very simply by implementing limiting values of tractions, $t_{i,lim}$ (axial friction, end-bearing resistance or lateral pressure) for each element. Alternatively, a more gradual reduction in shear modulus, G (or Young's modulus) may be adopted, such as the hyperbolic relationship (Basile 2003, 2013):

$$\frac{G}{G_0} = 1 - \left(\frac{R_f t_i}{t_{i,lim}} \right)^2 \quad (1)$$

where G_0 is the initial shear modulus at $t_i = 0$, and R_f is a hyperbolic factor limited to between 0 and 1. This delays decoupling of the pile from the rest of the group and also tends to even out the load distribution among piles in the group at operational loading levels, hence moderating the tendency for purely elastic analysis to concentrate loads towards the edges and corners of a pile group. From a design perspective, it may be appropriate to apply a material factor to the true ultimate values of tractions, $t_{i,ult}$, imposing limiting values $t_{i,lim}$ that are less than $t_{i,ult}$.

Modern computing power has now made full 3-dimensional finite element analysis a realistic approach, at least in the later stages of design. This has the advantage of allowing more sophisticated modeling of the soil response and has been used extensively in the design of piled rafts (Katzenbach et al. 2000, Reul and Randolph 2003). Clearly much greater computational resources are needed relative to BEM (or other 'elastic') based analyses, but 3D finite element analysis provides the most rigorous approach, obviating the need for simplifying assumptions such as that in Eq. (1).

At the opposite extreme, analysis using a 'lumped' pile response together with interaction factors between each pile offers the fastest approach, which is ideal for initial stages of design. This approach is used in the software PIGLET, which originated in 1980 (a version that formed the basis of MPILE), but has been improved over the intervening years (Randolph 2003, 2019). The most recent (2019) version, presented here for the first time, allows simulation of non-linear (pre-failure) axial and lateral response of individual piles in addition to a limiting axial capacity.

Hybrid approaches for pile group analysis have also been developed, whereby the response of individual piles are represented by non-linear axial and lateral load transfer curves, with interaction quantified using either the Mindlin elastic continuum solution (e.g. O'Neill et al. 1982), or load transfer modifying functions of some form (e.g. GROUP, Ensoft Inc).

The above methods for pile group analysis generally assume a rigid pile cap, with either pinned, fixed (with respect to rotation relative to the pile cap) or rotationally restrained connections between each pile head and the pile cap. However, in practice some flexing of the pile cap will occur, allowing differential settlement across the cap. Also, if the pile cap is cast directly on reasonably competent ground, the proportion of the load transferred directly from pile cap (i.e. raft) to the soil may be taken into account. Indeed, in extreme cases the piles may be viewed merely as a means to modify settlement of a primarily raft foundation (Burland et al. 1977, Randolph 1994). In that case, it is acceptable for the piles to reach their ultimate capacity, provided the raft provides

sufficient bearing capacity to satisfy relevant ultimate limit state conditions. It may be noted that, while the raft may contribute significantly to the overall stiffness of the piled raft foundation with respect to vertical loading, it generally has negligible contribution to the horizontal stiffness (e.g. Small and Zhang 2002).

A summary of some (but by no means all) of the software available for pile group analysis is provided in Table 1. The piled raft analysis tools may also be applied to pile groups by switching off raft-soil interaction. However, in most cases they are restricted to purely vertical loading. In addition to these ‘purpose-developed’ software, three-dimensional finite element analysis has become relatively widely used for the design of piled rafts and pile groups, as mentioned earlier.

Table 1 Summary of software for pile group and piled raft analysis

| Pile groups | Basic approach | Soil model | Interaction | Loading |
|----------------------|--------------------------------|---|----------------------------|---------------------------------|
| REPUTE (PGROUPn) | BEM | Layered (approximate) Non-linear, limiting capacity | Elastic - Mindlin | Vertical only Rigid pile cap |
| CLAP, DEFPIG | BEM | Layered (approximate) Non-linear, limiting capacity | Interaction factors | General 3D Rigid pile cap |
| PIGLET | Analytical | Linearly varying modulus Non-linear, limiting capacity | Semi-analytical | General 3D Rigid pile cap |
| GROUP, PILGRP1 | Load transfer curves | Layered Non-linear, limiting capacity | Load transfer modifiers | General 3D Rigid pile cap |
| Piled rafts | | | | |
| Zhang & Small (2000) | Finite layer | Layered Elastic, limiting capacity | Elastic | General 3D Flexible raft |
| NAPRA | BEM | Layered (approximate) Non-linear, limiting capacity | Interaction factors | Vertical only Flexible raft |
| GARP | BEM | Layered (approximate) Elastic, limiting capacity | Interaction factors | General 3D Flexible raft |
| HyPR | Semi-analytical and elastic | Linearly varying modulus Elastic, limiting capacity | Elastic - Mindlin | Vertical only Flexible raft |

The paper presents one or two comparisons of results obtained from some of these tools, demonstrating a relatively high level of agreement. Two particular aspects are then looked at in more detail. The first is the incorporation of non-linear response of individual piles in the group, and its influence on the overall pile group stiffness and internal load sharing among the piles. The second is the rather important question of differential settlement, where an iterative approach is explored to assess the extent to which simple analysis tools such as PIGLET may be linked manually to raft analysis software in order to assess load sharing between raft and pile groups and the differential settlements across the raft.

2. HIERACHICAL APPROACH

2.1 Lumped Models for Complete Pile Group and Raft

Mandolini et al. (2017) described in some detail a simple approach to the design of piled rafts, whereby the separate responses of the pile group and raft may be represented by ‘lumped’ non-linear functions of the loads, Q_p and Q_r , relative to their respective capacities, $Q_{p,ult}$ and $Q_{r,ult}$. These may then be combined to form the overall piled raft response. Generic functions for the tangent stiffnesses of pile group and raft took the form:

$$\frac{dQ_p}{dw_p} = K_{p,t} = K_{p,0} \left(1 - \frac{Q_p}{Q_{p,ult}} \right)^{np} ; \quad \frac{dQ_r}{dw_r} = K_{r,t} = K_{r,0} \left(1 - \frac{Q_r}{Q_{r,ult}} \right)^{nr} \quad (2)$$

where: dw_p, dw_r = incremental pile group and raft settlements

$K_{p,t}, K_{p,0}, K_{r,t}, K_{r,0}$ = tangent and initial stiffness of pile group and raft, respectively

n_p, n_r = adjustable powers to reflect a given degree of non-linearity.

The incremental response of the piled raft may then be obtained from (Randolph 1983, Clancy and Randolph 1993):

$$\begin{Bmatrix} dw_p \\ dw_r \end{Bmatrix} = \begin{bmatrix} 1/K_{p,t} & \alpha_{pr}/K_{r,0} \\ \alpha_{rp}/K_{p,0} & 1/K_{r,t} \end{bmatrix} \begin{Bmatrix} dQ_p \\ dQ_r \end{Bmatrix} \quad (3)$$

The leading diagonal terms represent the tangent stiffness of pile group and piled raft respectively, while the trailing diagonal represents the raft-soil-pile interaction, which is based on the initial elastic stiffness – the principle proposed by Caputo and Viggiani (1984) (see also Randolph 1994). Symmetry was imposed, replacing $\alpha_{pr}/K_{r,0}$ by $\alpha_{rp}/K_{p,0}$. For relatively large pile groups, the interaction factor, α_{rp} , was found to trend towards a value of 0.8 (Clancy and Randolph 1993).

Although lumped pile group and raft models such as the above are adequate to represent the response of a piled raft, they are somewhat limited in respect of quantifying the load distribution among the piles in the group, or the effects of bending of the raft. Also, the appropriateness of the interaction relationship of Eq. (3) becomes questionable as the load carried by either component approaches its ultimate value.

2.2 Non-Linear Models for Single Piles

The non-linear response expressed in Eq. (1) acts at the soil element (or pile-soil traction) level, whereas Eq. (3) acts at the opposite extreme of the complete pile group and raft units. Between these lie approaches that model the non-linear response of each pile, which are useful for software where the pile response is represented analytically. For example, PIGLET uses analytical solutions of Randolph and Wroth (1978) for the axial response at the pile head, and Randolph (1981) for the lateral response.

For the axial response, the initial pile head stiffness $k_{v,0}$ is modified for non-linear analysis using a generalized hyperbolic expression relating the current *secant* stiffness k_v to the axial load P normalized by the imposed limiting axial capacity V_{lim} :

$$\frac{k_v}{k_{v,0}} = 1 - f \left(\frac{V}{V_{lim}} \right)^g \quad (4)$$

Two parameters f and g allow a wide range of non-linear forms to be represented, with the reduction in secant stiffness given by $1 - f$ and the parameter g changing the curvature, as shown in Fig. 1a.

Under lateral loading, it is often not really possible to identify a (geotechnical, as opposed to structural) capacity and so it is more convenient to define the reduction in stiffness in terms of the

elastic pile head displacement $u_{0,el}$ normalized by the value at which the secant stiffness reduces by 50%, $u_{0,50}$. The expression adopted in PIGLET is

$$\frac{k_h}{k_{h,0}} = \frac{1}{1 + \left(\frac{u_{0,el}}{u_{0,50}} \right)^p} \quad (5)$$

As shown in Fig. 1b, high values of the power p will provide an almost elastic, perfectly plastic response, with a limiting horizontal load of $H_{ult} \sim k_{h,0}u_{0,50}$. By contrast, lower values will give gradually decreasing degrees of non-linearity.

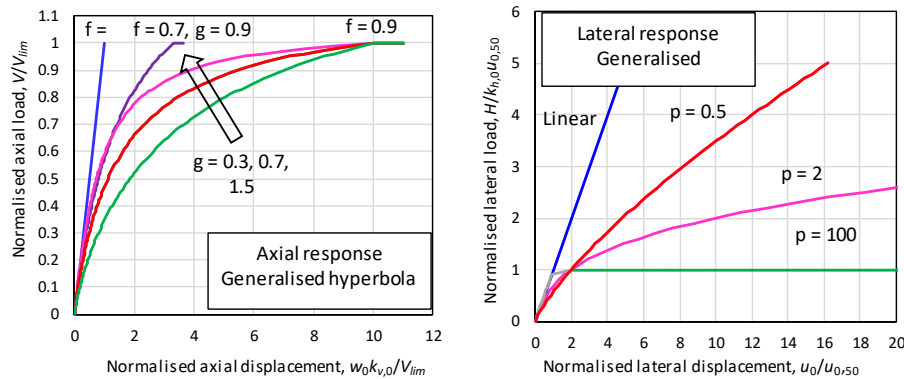


Fig. 1 Example non-linear relationships for (a) axial and (b) lateral response

With respect to interaction between piles, the same principle is followed as for the piled raft system discussed earlier. That is, the displacement of a neighboring pile is assumed proportional to the *elastic* displacement of the loaded pile. In PIGLET, interaction relationships are expressed analytically by means of expressions derived on the same basis as for the single pile (elastic) stiffness (axial interaction), or based on results from finite element analysis (lateral interaction).

The non-linear relationships given in Eqs. (4) and (5) are phenomenological in nature and the non-linear parameters need to be assessed in the light of load test data, or alternatively based on experience or more sophisticated numerical analysis of the single pile response, for example using load transfer analysis software such as RATZ (Randolph 2003), LAP (Doherty 2018) or LPILE (Ensoft 2016). Examples where field data are available for both single pile response and pile group response are considered later.

3. EXAMPLE COMPARISONS OF PILE GROUP RESPONSE

3.1 Non-linear axial response of pile groups

A useful comparison of different software for pile group analysis was provided by Pirrello and Poulos (2014), who considered two different pile groups: a small 3×3 group and a larger 172 pile group, both subjected to full 3-dimensional loading. Details of the 3×3 group are shown in Fig. 2, and key results are summarized in Table 2. Young's modulus for the pile was taken as 30,000 MPa while a uniform value of 50 MPa was assumed for the soil, but with an increase to 60 MPa at pile tip level (depth of 15 m). The pile cap was level with the ground surface but non load bearing.

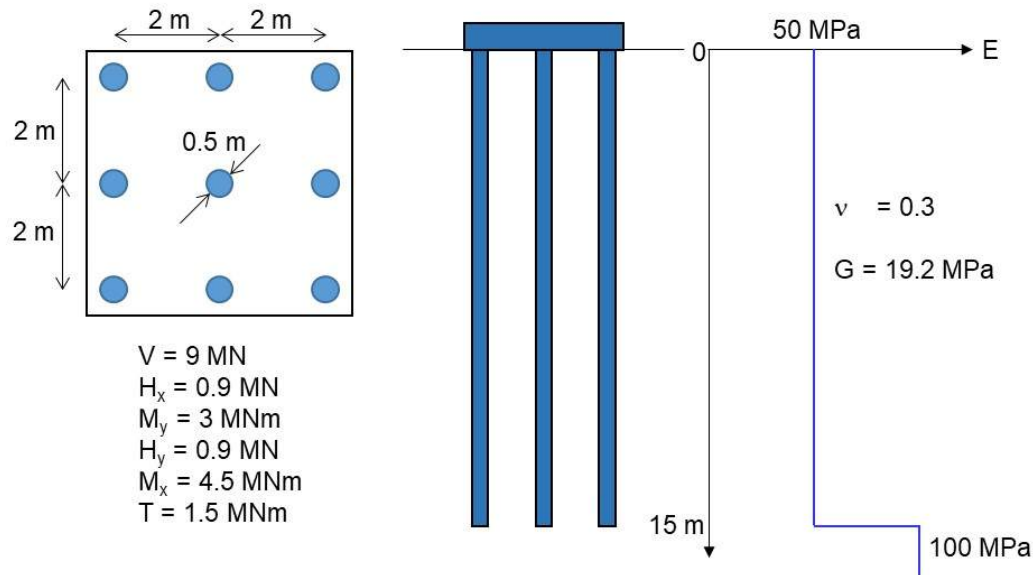


Fig. 2 Example 9-pile group considered by Pirrello & Poulos (2014)

Table 2 Results for 9-pile group (Pirrello & Poulos 2014)

| Quantity | Units | CLAP | PIGLET ¹ | REPUTE | PLAXIS |
|--------------------------|----------|------|---------------------|--------|--------|
| Central settlement | mm | 7.43 | 9.4 | 8.8 | 14.1 |
| Lateral deflection (x) | mm | 3.1 | 2.9 | 3.3 | 4.7 |
| Lateral deflection (y) | mm | 3.2 | 3.0 | 2.3 | 4.2 |
| Rotation (about y axis) | mradians | 0.4 | 0.4 | 0.2 | 3.2 |
| Rotation (about x axis) | mradians | 0.5 | 0.6 | 0.6 | 1.9 |
| Torsional rotation | mradians | 0.4 | 0.4 | 0.5 | - |
| Maximum axial load | MN | 1.9 | 1.9 | 1.8 | 1.8 |
| Maximum lateral load (x) | MN | 0.17 | 0.19 | 0.25 | 0.27 |
| Maximum lateral load (y) | MN | 0.17 | 0.19 | 0.25 | 0.26 |
| Maximum moment (x:z) | MNm | 0.12 | 0.12 | 0.18 | 0.32 |
| Maximum moment (y:z) | MNm | 0.11 | 0.10 | 0.14 | 0.31 |
| Maximum torque | MNm | 0.01 | 0.01 | 0.01 | - |

Note¹: Corrected results; Pirrello & Poulos published results for PIGLET were incorrect

Results for the three pile group analysis software, CLAP (Coffey 2017), PIGLET and REPUTE showed remarkable consistency, in terms of both the (rigid) pile cap deflections and rotations, and also the extreme loads within the group. REPUTE tended to show higher maximum lateral loads and moments compared with the other two programs, possibly due to modelling shielding effects within the group under lateral loading (Basile 2003). Interestingly, however, the PLAXIS analysis gave much greater vertical and lateral deflections (some 50% greater than the average of the pile group programs), and also extremely high rotations. Pirrello and Poulos (2014) do not comment on these much greater deflections and rotations from PLAXIS, but they are certainly of some concern since 3-dimensional finite element analysis is generally assumed to provide the most rigorous form of analysis. On the other hand, however, it seems unlikely that all three of the pile group programs are that much in error, as all have been well validated against rigorous analyses.

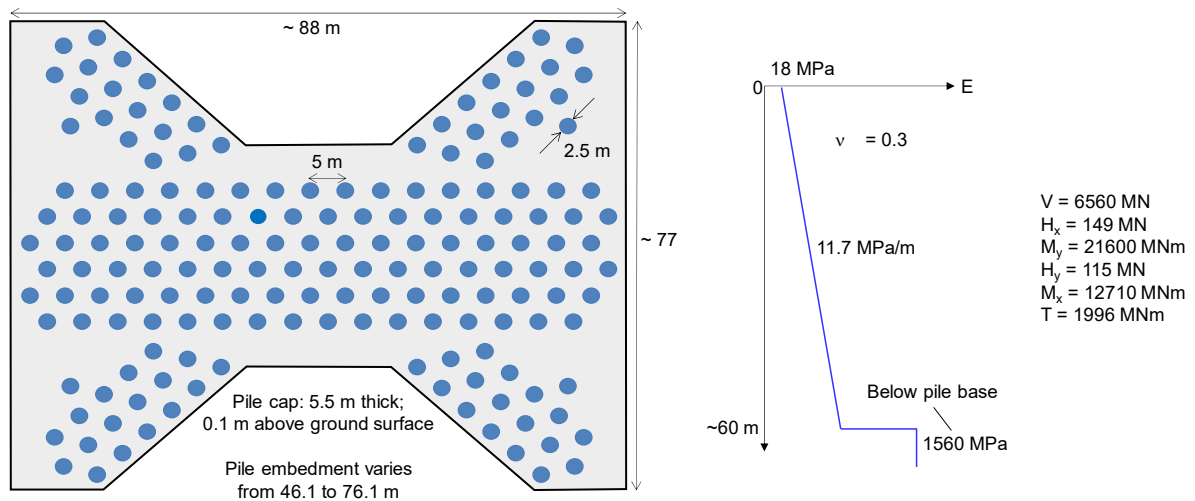


Fig. 3 Pile foundations for Incheon Tower considered by Pirrello & Poulos (2014)

Table 3 Results for Incheon Tower foundations (Pirrello & Poulos 2014)

| Quantity | Units | CLAP | PIGLET ¹ | | | REPUTE | PLAXIS |
|--------------------------|----------|------|---------------------|------|------|--------|--------|
| | | | E | E-P | NL-P | | |
| Central settlement | mm | 53.0 | 56.7 | 58.7 | 69.7 | 55.0 | 56.0 |
| Lateral deflection (x) | mm | 18.5 | 19.5 | 19.8 | 20.4 | 21.0 | 18.7 |
| Lateral deflection (y) | mm | 14.9 | 15.0 | 15.3 | 16.4 | 18.0 | 15.0 |
| Rotation (about y axis) | mradians | 0.2 | 0.2 | 0.2 | 0.3 | 0.2 | 0.2 |
| Rotation (about x axis) | mradians | 0.2 | 0.1 | 0.2 | 0.3 | 0.0 | 0.2 |
| Torsional rotation | mradians | 0.4 | 0.1 | 0.1 | 0.1 | 0.3 | 0.3 |
| Maximum axial load | MN | 84.6 | 140.6 | 83.5 | 69.4 | 84.8 | 83.0 |
| Maximum lateral load (x) | MN | 2.7 | 4.2 | 4.2 | 3.9 | 3 | 2.5 |
| Maximum lateral load (y) | MN | 2.6 | 3.1 | 3.1 | 2.9 | 2.8 | 2.2 |
| Maximum moment (x:z) | MNm | 22.9 | 18.9 | 18.7 | 16.4 | 21.4 | 20.0 |
| Maximum moment (y:z) | MNm | 22.9 | 13.8 | 13.4 | 11.3 | 18.5 | 21.0 |
| Maximum torque | MNm | 3.7 | 0.5 | 0.5 | 0.5 | 1.0 | 2.5 |

Note¹: For PIGLET, three sets of results are shown: (a) Purely elastic (E); (b) Elastic but with a limiting axial load of 83.5 MN imposed for every pile (E-P); and (c) Non-linear axial and lateral responses, for the same ultimate pile axial capacity of 83.5 MN

The second example considered by Pirrello and Poulos (2014) was for the 172-pile foundations for the proposed Incheon Tower (see also Abdelrazaq et al. 2011), as illustrated in Fig. 3. The geological conditions are quite complex, and the 2.5 m diameter bored piles ($E_p = 39,000$ MPa) piles were designed to be founded into unweathered rock at tip levels varying between 46.1 m and 76.1 m. A simplified linearized profile of soil modulus was adopted for the PIGLET analyses (consistent with the profile adopted by Pirrello and Poulos (2014) – private communication), with Young's modulus increasing with depth at a rate of 11.7 MPa/m from a surface value of 18 MPa. The Young's modulus of the unweathered rock below pile tip level (regardless of the actual depth) was assumed to be 1560 MPa.

Comparative results obtained using the three pile group analysis programs, CLAP, PIGLET and REPUTE, are summarized in Table 3, together with results from a 3-dimensional finite element analysis using PLAXIS. For PIGLET, three sets of results are shown, corresponding to linear elastic soil response (E), elastic soil response but allowing for axial failure (E-P) at an ultimate capacity of 83.5 MN (an average of those resulting from limiting pile-soil tractions imposed in CLAP, REPUTE and PLAXIS), and non-linear axial and lateral soil response (NL-P) with the same ultimate pile axial capacity of 83.5 MN carried out with the new enhanced version of PIGLET (Randolph, 2019). Non-linear soil parameters of $f = g = 0.9$, $u_{0,50} = 0.02d_p = 50$ mm, where d_p is the pile diameter, and $p = 0.8$ (Eqs (4) and (5)) were adopted.

Extremely consistent results were obtained from all sets of analysis, both for deflections and rotations, and also for extreme loads carried by piles close to the corners of the foundation. For the purely elastic PIGLET analysis (the only elastic analysis), the maximum axial load is considerably higher. However, by limiting the maximum load to 83.5 MN, but still with elastic soil response (E-P case), the pile group deflections remain virtually unchanged. For the non-linear case, the vertical deflection at the centroid of the pile group increases by about 20%. Interestingly, although the lateral stiffness of each pile reduces by a factor of 1.5 (for $u_{0,el}/u_{0,50}$ of ~ 0.4), this has negligible effect on the lateral deflections of the pile cap because the lateral stiffness of the whole pile group is dominated by interaction effects. What is noticeable, however, is that the non-linear analysis gives rise to considerably more uniform distribution of the loads within the pile group, so that the extreme axial and lateral pile loads decrease by around 20% (axial) and 10% (lateral).

3.2 Comparisons with field data – load testing of small pile groups

Some comparisons are provided with results of field tests where single piles and pile groups were loaded either vertically or horizontally. The first two cases involve vertical loading of relatively small pile groups comprising either nine piles (O'Neill et al. 1980, 1982) or five piles (McCabe and Lehane 2006), summary details of which are presented in Fig. 4 and Fig. 5 respectively.

In addition to the load test on the nine pile group, O'Neill et al. (1982) reported results from a load test carried out on an independent single pile installed in the vicinity of the pile group. In back-analysis of these tests, they adopted a uniform Young's modulus value for the soil of 158 MPa, together with Poisson's ratio of 0.5. In both cases the loads were applied at a distance of 0.9 m above ground level.

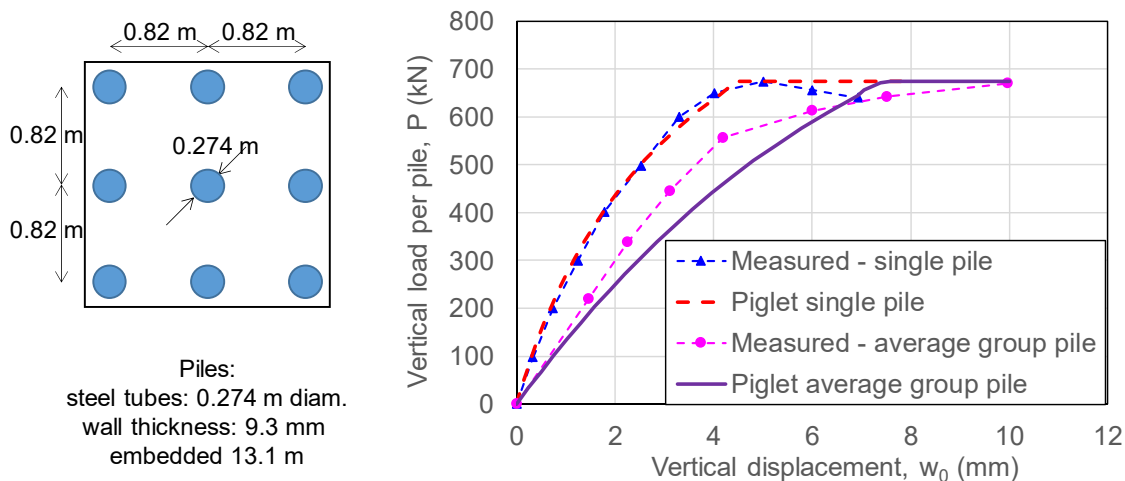


Fig. 4 Layout and vertical load response of nine pile group (O'Neill et al. 1982)

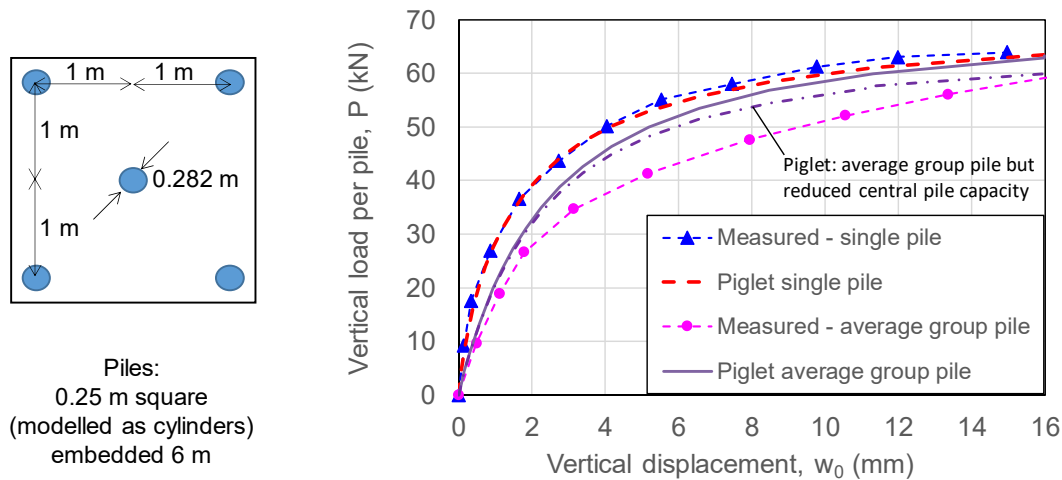


Fig. 5 Layout and vertical load response of five pile group (McCabe and Lehane 2006)

Here a better fit was obtained using a linearly varying Young's modulus, from 50 MPa at ground level to 550 MPa at the level of the pile tips. Non-linear soil parameters of $f = 0.6$ and $g = 0.85$, together with a limiting axial capacity of 674 kN, led to a reasonably good fit to the single pile load test, with initial stiffness of 470 kN/mm and a non-linear settlement component of 3.3 mm at failure (Fig. 4). The corresponding results from PIGLET for the nine pile group matched the initial stiffness of 140 kN/mm (30% of the single pile value) well. However, the field test data showed rather smaller non-linear components of settlement for loads up to 550 kN per pile compared with the simulated response.

The five pile group reported by McCabe and Lehane (2006) comprised driven precast concrete piles (Young's modulus taken as 40,000 MPa), with corner piles placed on a 2 m square grid. The load tests were simulated taking a soil shear modulus of 10 MPa (uniform with depth), as reported by Sheil et al. (2018), Poisson's ratio of 0.45, and non-linear parameters of $f = 0.96$ and $g = 0.4$. The piles were modelled by equivalent cylindrical piles, diameter 0.282 m, giving a center to corner spacing of 2.5 diameters. The ultimate axial capacity of each pile was taken as 64 kN.

As shown in Fig. 5, the single pile response is well matched by PIGLET, but the simulated group response is rather stiffer than measured in the field test. The load-settlement response of each corner pile (loaded through an essentially rigid pile cap resting on a 50 mm layer of polystyrene laid on the ground) was relatively similar, but the center pile showed a much softer response, reaching a load of just under 48 kN at a pile cap settlement of 25 mm (McCabe and Lehane 2006). However, even adopting this lower capacity for the center pile makes relatively little difference to the simulated group response. One possible explanation for the much greater non-linearity of the pile group in the field lies in the effects of installation. McCabe and Lehane mentioned that the center pile, which was driven first, was lifted 5 mm during driving of the corner piles; if something similar also happened for the corner piles during driving of each subsequent pile, then mobilization of the base capacities would have required greater settlements, hence increasing the degree of non-linearity in the overall group response.

On the face of it, these two comparisons of the field and simulated responses of single piles and pile groups show contrasting fits to the measured group responses, with over-estimation of non-linearity for the nine pile group, and under-estimation for the five pile group. However, in both cases the quality of match at a typical operation load of around 30 to 40% of the group capacity is reasonable, illustrating the approach of first matching the single pile response (either predicted independently or obtained from load tests) in order to estimate the pile group response.

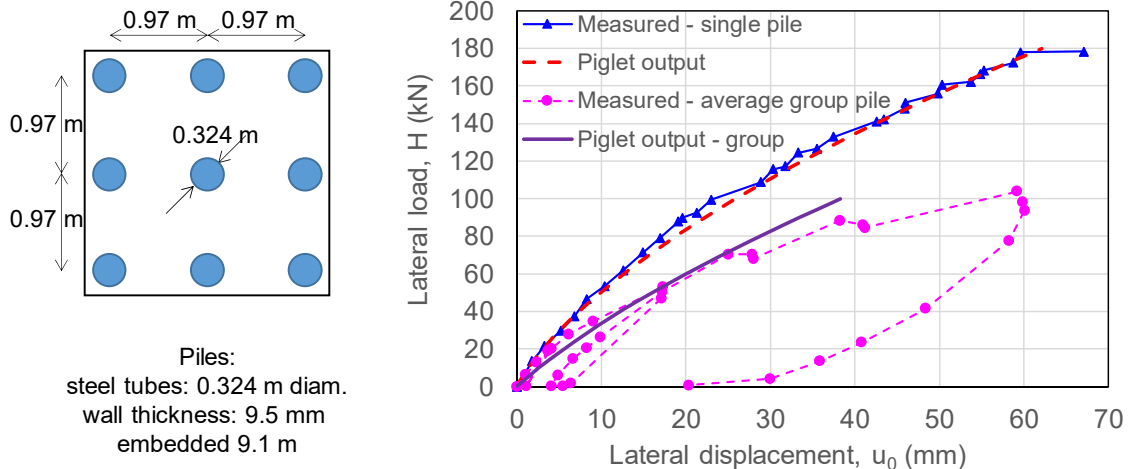


Fig. 6 Layout and lateral load response of nine pile group (Rollins et al. 2006)

The last case study of load tests on small groups of piles is that reported by Rollins et al. (2006), for lateral loading of a nine pile group (see Fig. 6). The 0.324 m diameter steel pipe piles have equivalent Young's modulus (for a solid pile) of about 23,000 MPa for axial loading, and 43,000 MPa for lateral loading. The piles were loaded at a height of 0.44 m above ground level, using a grid system that gave effectively pinned conditions for the pile heads at that level. The soil conditions are reported by Rollins et al. (1998) as comprising interbedded desiccated clayey silt and sand layers, with shear wave velocities of 120 to 150 m/s (so small strain shear modulus of 26 to 40 MPa assuming a unit density of around 1.8 t/m³).

Here the single pile response has been matched using a uniform shear modulus of 10 MPa (Poisson's ratio of 0.3), and non-linear soil parameters of $u_{0,50} = 0.02d_p = 6.5$ mm and a power of $p = 0.8$ (see Eq. (5)), which gives an excellent fit to the measured response. These parameters also allow a reasonable fit to the nine pile group response, as shown in Fig. 6. At loads above about 80 kN, where the pile head deflection reaches 10% of the pile diameter (but deflections at ground level about half that, so 5% of the diameter), the measured group response starts to soften relative to the PIGLET curve. This is probably due to increasing effects of 'shadowing', with the lateral resistance of any trailing pile lower than that of leading piles. Such effects were noted by Rollins et al. (1998), with typically each front row pile carrying ~14% of the load, compared with 10% for each middle row pile and 9% for each trailing edge pile.

3.3 Comparison with field performance – large vertically loaded pile group

The non-linear response of individual piles becomes of much lower significance for large groups of piles, where the group stiffness is dominated by interaction effects. An interesting case study was presented by Goosens and Van Impe (1991), where a large group of cast in situ piles were used to support a number of grain elevators (silos). The piles were embedded 13.1 m into relatively low density sands, which were underlain by tertiary clays (the diagonal hatched layers in Fig. 7a). The piles were 0.52 m in diameter and arranged on a rectangular 41 × 17 grid, with grid spacing of 2.08 m (four diameters). In order to allow for variability across the site, expanded bases of different size were constructed beneath each pile, although all piles were the same length. Here, a uniform base diameter of 0.8 m has been assumed (following Sheil et al. 2018).

Load tests on single piles gave very consistent responses, with an example shown in Fig. 7b (settlement scale on bottom horizontal axis). The ultimate capacity was estimated as about 4.9 MN, although load tests were only conducted to 2.25 MN. The fitted single pile response from PIGLET was obtained assuming a uniform shear modulus of 60 MPa, and non-linear parameters of $f = 0.95$ and $g = 0.7$. The calculated group response is also shown (settlement scale on top horizontal axis). The elastic group settlement ratio is 37.5, resulting in a relatively small non-linear component of the virtually linear response.

The average applied load during operation of the silos was 1.3 MN per pile. The resulting settlement profiles calculated by PIGLET are shown in Fig. 7c, and compared with measured settlements along one edge of the silo slab taken two years after the start of operations. The agreement is reasonable. However, the long term settlements are more difficult to estimated, because of consolidation of the underlying clays. After some ten years of operation, the maximum settlements along the edge had exceeded 180 mm (Goosens and Van Impe 1991).

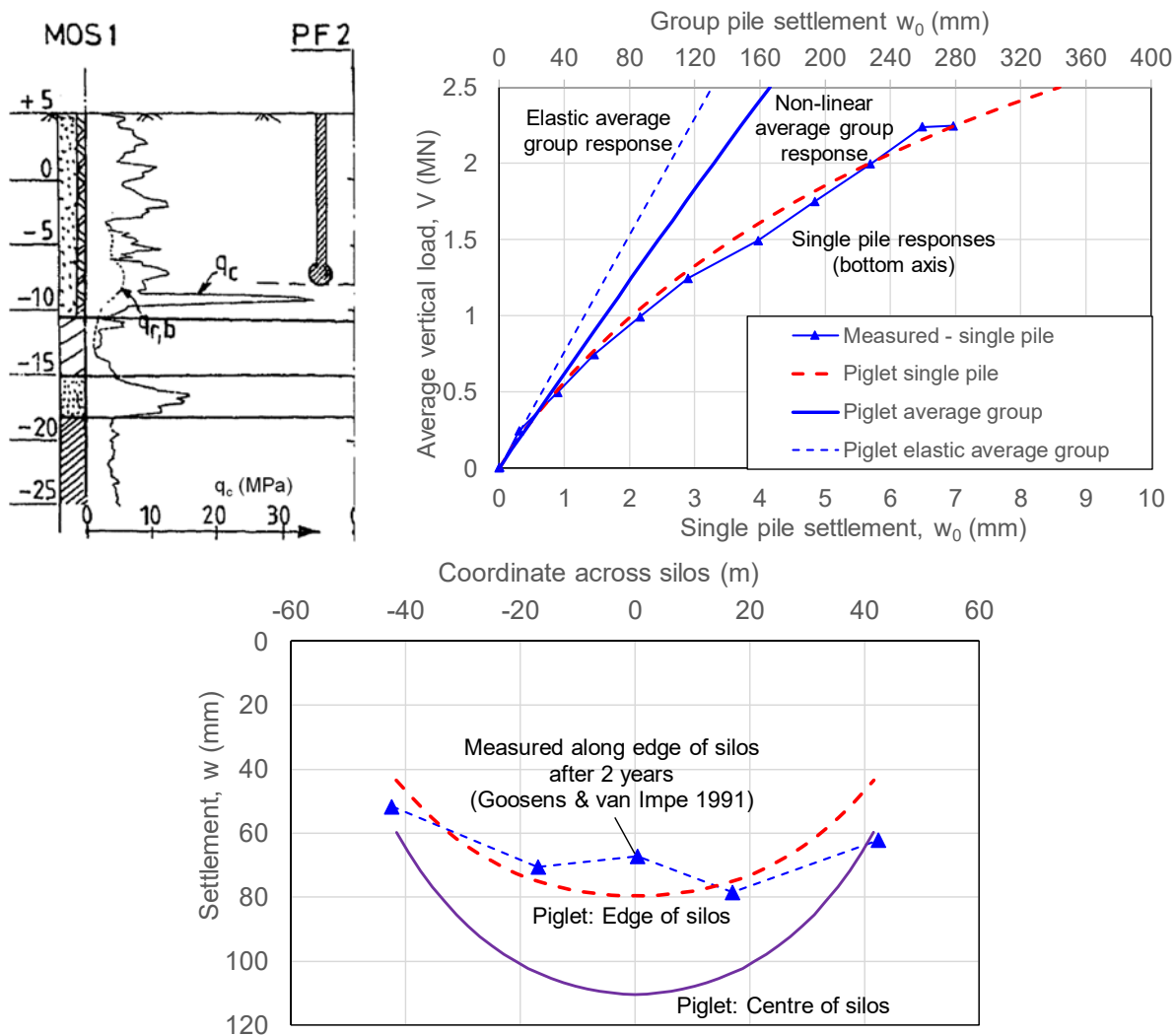


Fig. 7 Measured and simulated performance of silo foundations (Goosens and Van Impe 1991)
 (a) Example cone profile and stratigraphy, (b) Simulation of single pile load test and average group pile response, (c) Measured and simulated settlement profiles

4. PILED RAFTS

4.1 Non-linear analysis of pile groups with flexible pile cap

The assumption of a rigid pile cap, either free-standing or able to transfer load directly to the soil, will exacerbate the tendency for loads in the pile group to be concentrated towards the edges and corners of the pile group. As noted earlier, non-linear response of the piles for the Incheon foundation analyses led to significant reduction in the maximum axial load within the group by comparison with either a fully elastic analysis or an elastic-plastic analysis. For that study, where the applied vertical load was about 47% of the total axial pile capacity, pure vertical loading of the pile group (i.e. removing the horizontal and moment loading) would give a maximum load on the corner piles of 135 MN for elastic response, compared with an average applied load of $6560/172 = 38$ MN. So, the maximum load is 3.5 times the average load. However, for the non-linear model and an imposed pile capacity of 83.5 MN, the extreme load reduces by a factor of two to 66 MN (1.7 times the average applied load).

However, accounting for flexibility of the pile cap will contribute further to evening out of the pile loads, and also allow quantification of differential settlements across the pile cap, or raft. In addition to full 3D finite element analyses, several software tools have been developed over the last two or three decades that enable full piled raft analysis including representation of interactions between piles and between piles and raft. The earliest generation of these included HyPR (Clancy and Randolph 1993) and GARP (Poulos 1994, 2001). These were restricted to purely vertical loading and elastic soil response, but also allowed capping of axial loads (or pile-soil tractions) to limit the pile capacity. More recent tools include NAPRA (Russo 1998, Russo et al. 2012), a finite layer approach (Small and Zhang 2002) and an enhancement of GARP combining BEM and finite layer analysis (Small and Poulos 2007, Poulos et al. 2011).

The state of the art of piled raft analysis now allows vertical and horizontal loading, together with non-linear response for pile-soil tractions and raft-soil interactions, but maintaining purely elastic interactions between ‘off-diagonal’ terms of the stiffness matrices. This level of sophistication is therefore approaching the ‘gold standard’ of 3D non-linear finite element analysis using commercial products such as ABAQUS and PLAXIS.

Purpose-developed software for piled raft analysis is relatively sparse, but there is rather more software available for analysis of either pile groups alone, or shallow raft foundations. The following sections discuss an iterative approach that aims to achieve a compatible sets of pile loads and pile head settlements with the corresponding sets for the raft. The approach is illustrated using PIGLET for the pile group (but restricted to elastic response only) and a finite element code to model the raft and the soil as an elastic half-space, but in principle the approach may be used with any pairs of pile group and raft analysis tools.

4.2 Piled-raft analysis using the iterative approach

4.2.1 General description of the iterative approach

The iterative approach for piled rafts comprises two complementary analyses, namely PIGLET and a raft analysis, iterating between:

- Analysis of the pile group under consideration of the pile-pile interaction.
- Analysis of a raft placed on an elastic continuum with the piles modelled as elastic springs (Fig. 8).

So far, the iterative approach does not consider effects of pile-raft interaction. The raft and the elastic continuum are modelled by means of finite elements which allows consideration of the load

distribution on the raft and local variations of the raft stiffness (e.g. sections with different raft thickness). In the scope of this paper all raft-analyses for the iterative approach have been carried out with the finite element code TOCHNOG (Tochnog, 2019).

The iteration process can be summarized as follows:

1. Model pile group with fully flexible cap (PIGLET):
Output: spring stiffness for unit load on each pile; settlements at each pile head.
2. Model raft on elastic continuum and elastic springs (raft-analysis):
Input: supporting spring stiffnesses from step (1) representing the piles;
Output: pile loads; settlements at each pile head.
3. Model pile group with fully flexible cap (PIGLET):
Input: pile loads from step (2);
Output: pile spring stiffnesses; settlements at each pile head.
4. Iterate around steps (2) and (3) until differences between the displacements at each pile head calculated with PIGLET and the raft analysis are small.

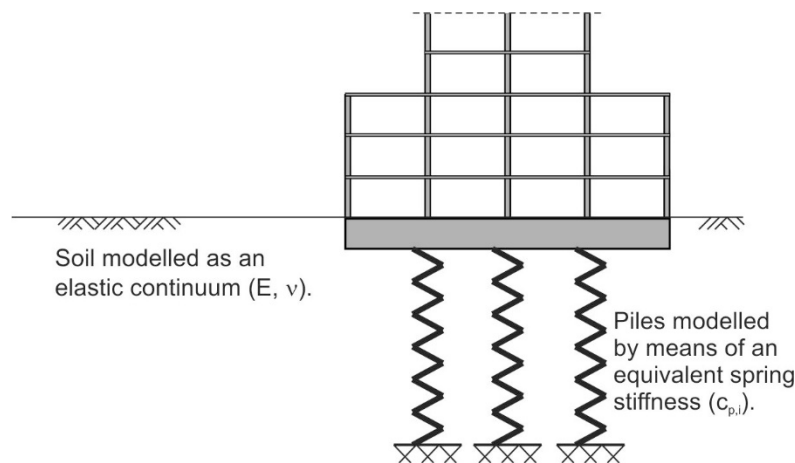


Fig. 8 Iterative approach: Model of the piled raft in the raft-analysis

4.2.2 Comparison of the iterative approach with 3D FEA

In this section the iterative approach is compared with the results of a numerical study on the bearing behavior of piled rafts presented by Reul (2004) (see Reul and Randolph 2004), applying 3D finite element analysis (3D FEA). The numerical study was carried out modelling subsoil conditions based on those in Frankfurt am Main, Germany, which is characterized mainly by tertiary soils and rock. They consist of Frankfurt clay at the top underlain by the rocky Frankfurt limestone. The Frankfurt clay is a stiff, overconsolidated clay with liquid limit, plastic index and natural moisture content very similar to the London clay (Butler, 1975). Sand and limestone bands of varying thickness are embedded in the Frankfurt clay, which results in a non-homogeneous appearance of the layer as a whole. The compressibility of the Frankfurt limestone, which is composed of massive limestone and dolomite layers, algal reefs, marly calcareous sands and silts and marly clay, is small compared with that of the Frankfurt clay.

In the finite element analyses the soil, which is in reality a multi-phase medium consisting of the three components solid phase (grains), liquid phase (pore water) and gaseous phase (pore air), was simplified to a single phase medium. The long term behavior of this simplified medium was characterized by drained shear parameters c' and ϕ' , with the non-linear material behavior modeled using an elastoplastic cap model. However, as the Frankfurt clay is overconsolidated, assuming a

maximum previous vertical stress of 450 kPa at its top surface, the analyses are dominated by the soil stiffness rather than the soil strength (Reul and Randolph 2003). The depth variation of the Young's modulus, E , of the Frankfurt clay is described by the following empirical formulation based on the back-analysis of boundary value problems in Frankfurt clay (Reul 2000):

$$E = 45 + 0.7 \left(\tanh \left(\frac{z - 30}{15} \right) + 1 \right) z \text{ MPa} \quad (6)$$

where z is the depth below the surface of the tertiary layers (m).

The raft and piles are considered as linearly elastic solids. A detailed discussion of the finite element analyses as well as the documentation of the applied soil parameters can be found in Reul (2004).

Fig. 9a shows the model conditions applied in the numerical study. The foundation level was set 14 m below ground level. The base of the Frankfurt clay, was set 83 m below ground level. For the comparison with the iterative approach a piled raft comprising $n = 49$ piles (length $L_p = 30$ m; diameter $d_p = 1.0$ m) was selected (Fig. 9b and c). The analysis with the iterative approach has been carried out for a load of $P = 360.9$ MN, which includes the weight of the raft.

In the analysis with the iterative approach the bottom of the model was equivalent to the bottom of the clay, i.e. the limestone with its significantly higher stiffness was treated as rigid. The material parameters applied for the iterative approach are summarized in Table 4. Please note that all analyses with the iterative approach presented subsequently in this paper (see Section 4.3) have adopted the soil stiffness profile expressed as Eq. (6). The simplified linearly varying shear modulus profile and base shear modulus required for the PIGLET analyses have been calculated from the Young's modulus profile and Poisson's ratio, taking account of the depth to limestone.

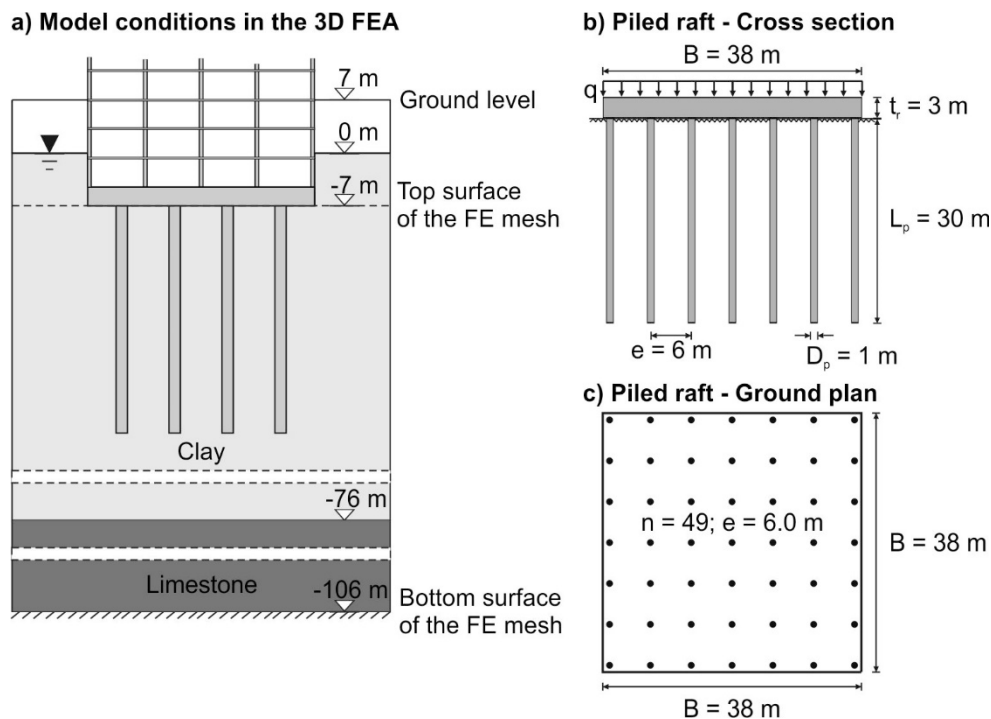


Fig. 9 Piled raft ($n = 49$; $L_p = 30$ m; $d_p = 1.0$ m): Configuration

Table 4 Piled raft ($n = 49$; $L_p = 30$ m; $d_p = 1.0$ m): Material parameters applied in the analysis with the iterative approach.

| Analysis | Parameter | | | | |
|---------------|--------------------------|------------------------|----------|---------------------|---------------------|
| PIGLET | Soil | Surface shear modulus | G_{0a} | [kPa] | $2.0320 \cdot 10^4$ |
| | | Shear modulus gradient | Gm_a | [kPa/m] | $4.361 \cdot 10^2$ |
| | Shear modulus below base | G_b | [kPa/m] | $6.8800 \cdot 10^4$ | |
| | Poisson's ratio | ν | [-] | 0.15 | |
| Raft analysis | Soil | Young's modulus | E | [MPa/m] | Equation (6)* |
| | | Poisson's ratio | ν | [-] | 0.15 |
| | Raft | Young's modulus | E | [kPa] | $3.0 \cdot 10^7$ |
| | | Poisson's ratio | ν | [-] | 0.20 |

* with depth of raft base below the surface of the tertiary layers $z_r = 7$ m

To quantify the performance of a piled raft, the ratio of the sum of all pile resistances, ΣR_{pile} to the effective settlement inducing load (settlement inducing load minus uplift), P_{eff} , may be expressed by a piled raft coefficient:

$$\zeta_{pr} = \frac{\Sigma R_{pile}}{P_{eff}} \quad (7)$$

A piled raft coefficient of unity indicates a freestanding pile group whereas a piled raft coefficient of zero signifies an unpiled raft.

Fig. 10a documents the development of the maximum and average settlements and the piled raft coefficient during the iteration process. The three parameters converge reasonably well with a difference between the 1st and 20th iteration of approximately 10 %. The settlement difference between raft and PIGLET analysis is less than 1 % after 10 iterations (average value) and 20 iterations (maximum value), respectively (Fig. 10b).

Fig. 11 compares the resistance-settlement response achieved with the 3D FEA and the iterative approach. While for a load of $P = 360.9$ MN ($= R_{tot}$) the 3D FEA gives a maximum settlement at the center of the raft of $s_c = 49$ mm, the iterative approach yields $s_c = 40$ mm. This tendency appears reasonable since 3D FEA and iterative approach both use the same elastic stiffness while for the 3D FEA additionally plastic deformations occur (although these are of course small at this load level). The share of the piles in the load transfer to the subsoil amounts to $\zeta_{pr} = 0.754$ (3D FEA) and $\zeta_{pr} = 0.636$ (iterative approach), respectively.

Fig. 12 shows a comparison of the normalized equivalent spring stiffness of the piles, $c^*_{pile,i}$, which is defined as

$$c^*_{pile,i} = \frac{c_{pile,i}}{\Sigma c_{pile,i}} \quad \text{with} \quad c_{pile,i} = R_i / s_i \quad (8)$$

where: $c_{pile,i}$ is the equivalent spring stiffness of pile i for a pile head settlement of s_i ,
 R_i is the pile resistance of pile i for a pile head settlement of s_i and
 $\Sigma c_{pile,i}$ is the sum of the spring stiffnesses of all 49 piles.

The agreement is reasonable, although the iterative approach still tends to overestimate the stiffnesses of piles towards the edges and corners of the raft compared with the 3D FEA. This may be due to non-linear soil response modelled in the latter, whereas the PIGLET analyses were only elastic (E-P in the notation of Table 3) for the iterative approach.

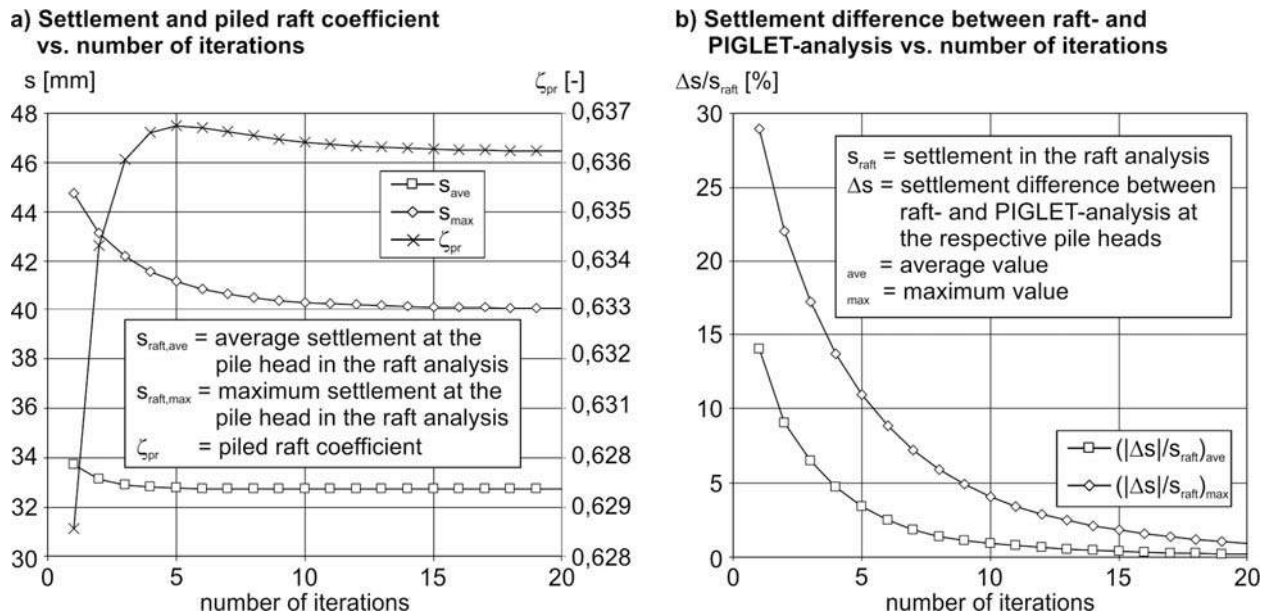


Fig. 10 Piled raft ($n = 49$; $L_p = 30$ m; $d_p = 1.0$ m): Progress of iteration approach

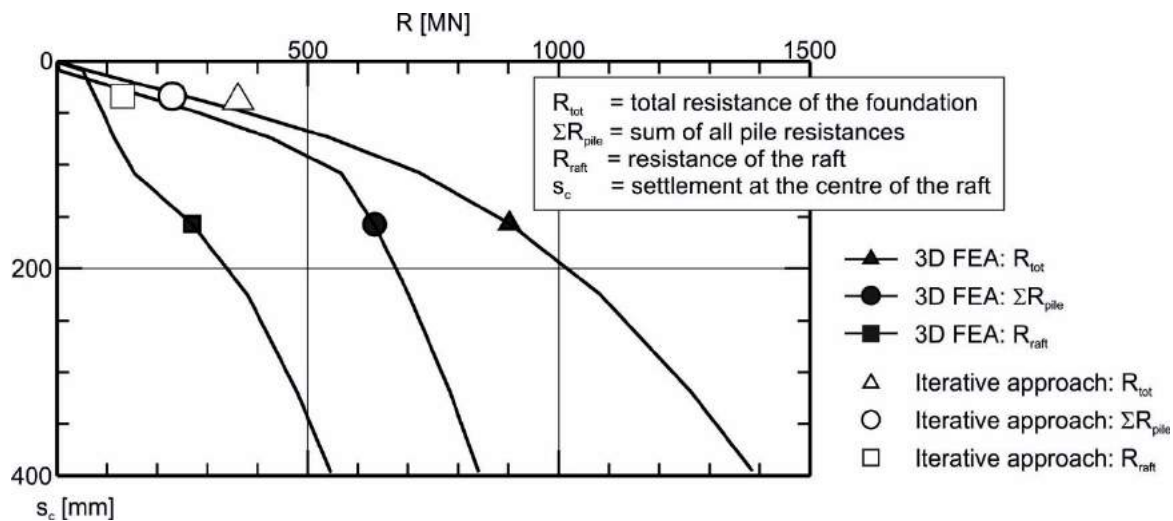


Fig. 11 Piled raft ($n = 49$; $L_p = 30$ m; $d_p = 1.0$ m): Resistance-settlement response

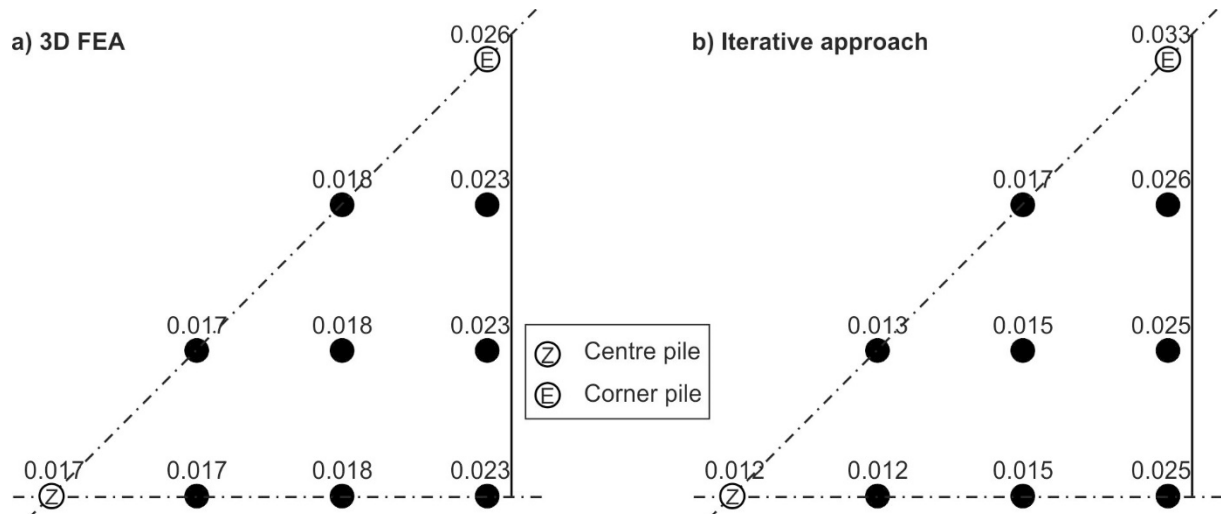


Fig. 12 Piled raft ($n = 49$; $L_p = 30$ m; $d_p = 1.0$ m): Normalized equivalent spring stiffness for the pile, $c^*_{pile,i}$, depending on the pile position

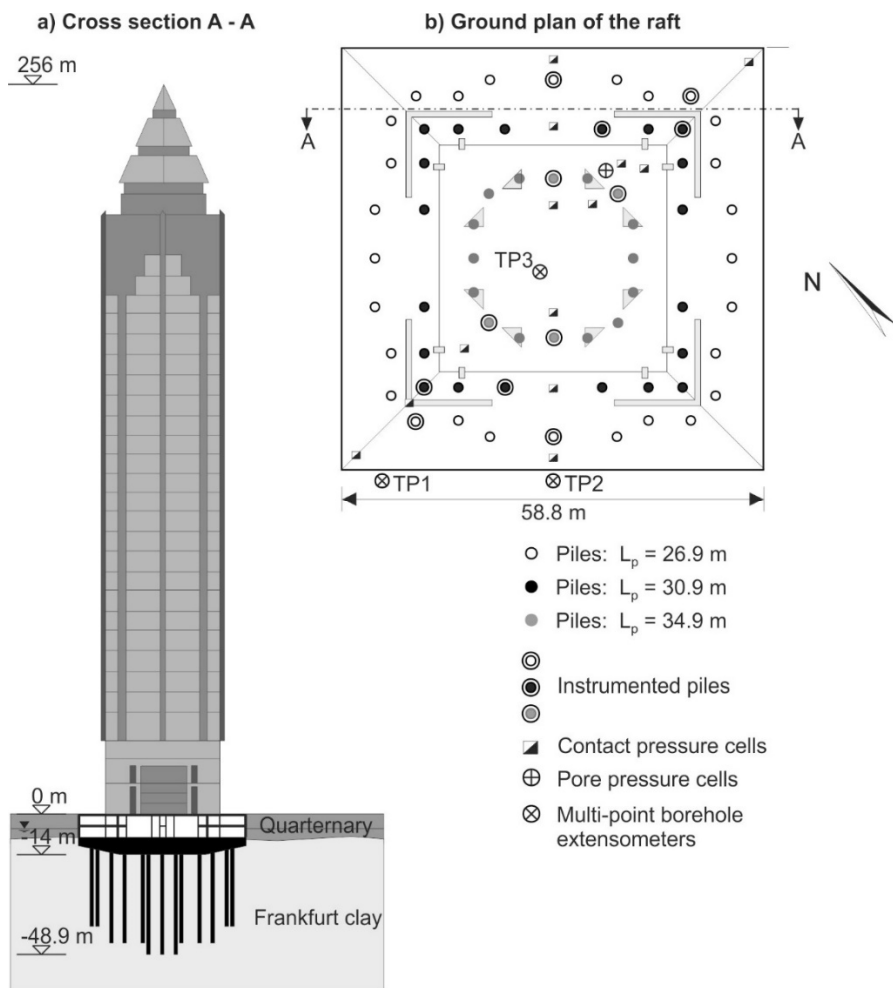


Fig. 13 Messeturm: Elevation and pile layout

4.3 Case studies

4.3.1 Messeturm (Frankfurt, Germany)

The piled raft of the 256 m high Messeturm comprises 64 bored piles and a square raft with an edge length of 58.8 m. The length of the 1.3 m diameter piles varies from $L_p = 26.9$ m (outer ring), $L_p = 30.9$ m (middle ring) to $L_p = 34.9$ m (inner ring). The foundation level of the 3 m to 6 m thick raft lies 11 m to 14 m deep below ground level (Fig. 13a). The construction of the building started in 1988 and was finished in 1991. The behavior of the foundation was monitored from the construction period until more than seven years after the building was finished by means of geodetic and geotechnical measurements with 12 instrumented piles, 13 contact pressure cells, 1 pore pressure cell and 3 multi-point borehole extensometers. The positions of the measurement devices are plotted in the ground plan of the raft (Fig. 13b).

In the vicinity of the Messeturm the subsoil consists of fill and quarternary sand and gravel up to a depth of 10 m below ground level, which is followed by the Frankfurt clay up to a depth of at least 70 m below ground level.

The groundwater level is situated 4.5 m to 5 m below ground level. During construction of a subway tunnel with a station 47 m east of the Messeturm, groundwater had to be drawn down more than 12 m at the tunnel (Sommer et al. 1991). As a result, the groundwater level in the vicinity of the Messeturm decreased by about 10 m, which led to a reduction of the uplift force on the raft of 287 MN. During the construction process of the subway tunnel and the station the groundwater lowering was suspended for 2 years and continued in 1994 until the end of 1996. The variation with time of the groundwater level and the average measured pile resistances for the inner, middle and outer pile ring are shown in Fig. 14. The changes in groundwater level, and the resulting uplift on the raft, caused alterations of the pile loads of up to 3 MN. Groundwater drawdown and rise are accompanied by increases and decreases of the pile loads, respectively.

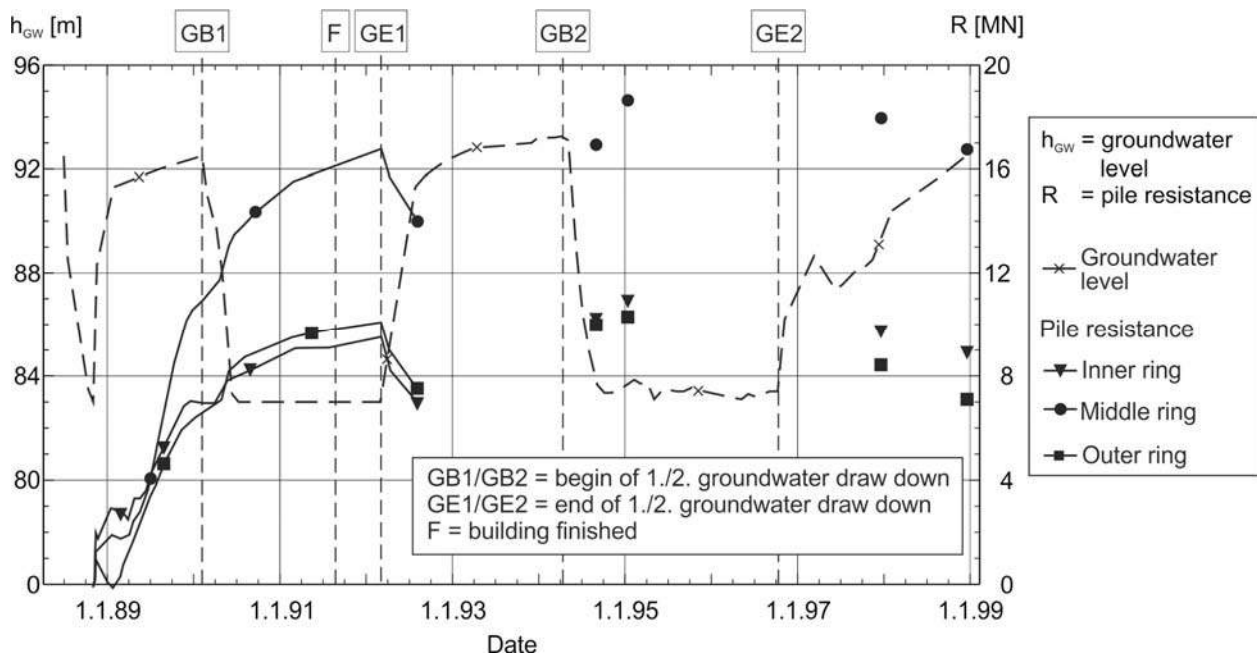


Fig. 14 Messeturm: Measured variation of groundwater level and pile resistance with time

Table 5 Messeturm: Material parameters applied in the analysis with the iterative approach.

| Analysis | Parameter | | | | |
|---------------|-----------------|--------------------------|----------|------------------|--------------------|
| PIGLET | Soil | Surface shear modulus | G_{0a} | [kPa] | $2.049 \cdot 10^4$ |
| | | Shear modulus gradient | Gm_a | [kPa/m] | $4.449 \cdot 10^2$ |
| | | Shear modulus below base | G_b | [kPa/m] | $4.291 \cdot 10^4$ |
| | | Poisson's ratio | ν | [-] | 0.15 |
| Pile | Young's modulus | E_{pa} | [kPa] | $3.0 \cdot 10^7$ | |
| Raft analysis | Soil | Young's modulus | E | [MPa/m] | Equation (6)* |
| | | Poisson's ratio | ν | [-] | 0.15 |
| Raft | Raft | Young's modulus | E | [kPa] | $3.0 \cdot 10^7$ |
| | | Poisson's ratio | ν | [-] | 0.20 |

* with depth of raft base below the surface of the tertiary layers $z_r = 5$ m

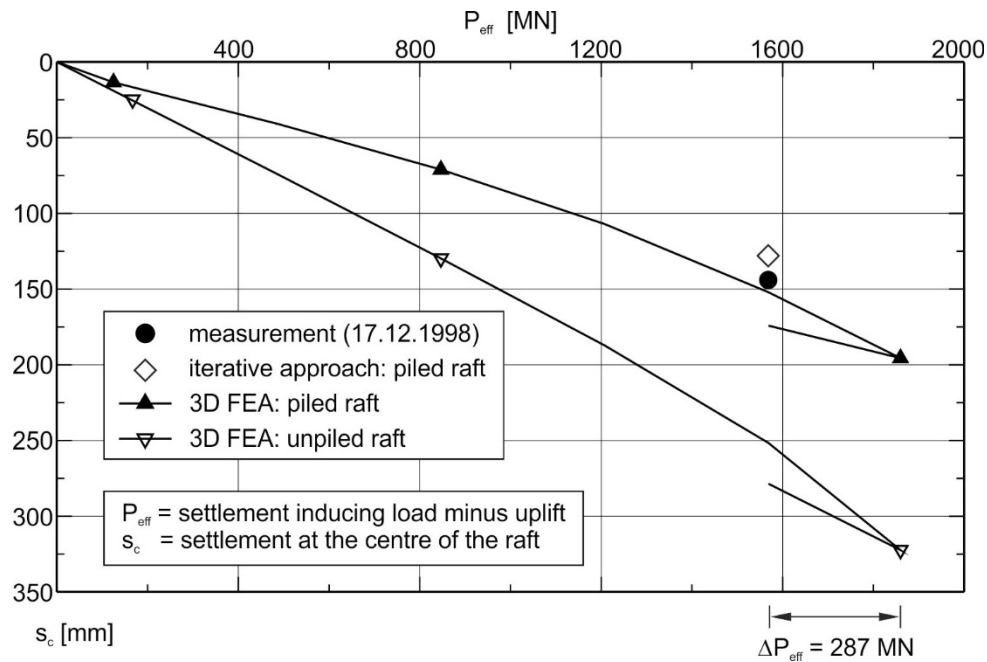


Fig. 15 Messeturm: Load-settlement response

The foundations of the Messeturm have been studied using 3D FEA with the soil model summarized in Section 4.2.2, and the calculated results have been compared with the in-situ measurements (Reul and Randolph 2003). The material parameters adopted are summarized in Table 5.

Fig. 15 compares the settlement at the center of the raft calculated with 3D FEA and the iterative approach with the last documented measurement in December 1998 (i.e. after the end of the 2nd groundwater drawdown), which corresponds to an effective settlement inducing load (change in superstructural load minus uplift) of $P_{eff} \approx 1569$ MN. It should be noted that the 3D FEA does not consider any time effects such as consolidation and creep, which therefore allows the results to be represented by a load-settlement curve. While the last documented measurement

gives a central settlement of 144 mm the calculated settlements at the center of the raft amount to 174 mm (3D FEA) and 128 mm (iterative approach), respectively. An additional 3D FEA carried out for an unpiled raft indicates that, with the piled raft, the settlement has been reduced to approximately 63 % of the settlement of the corresponding unpiled raft.

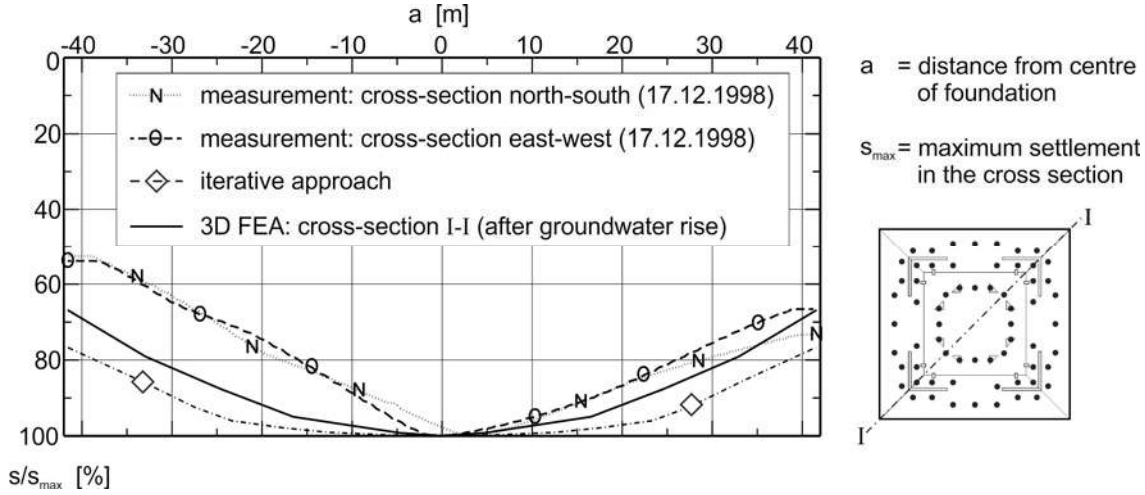


Fig. 16 Messeturm: Distribution of settlements

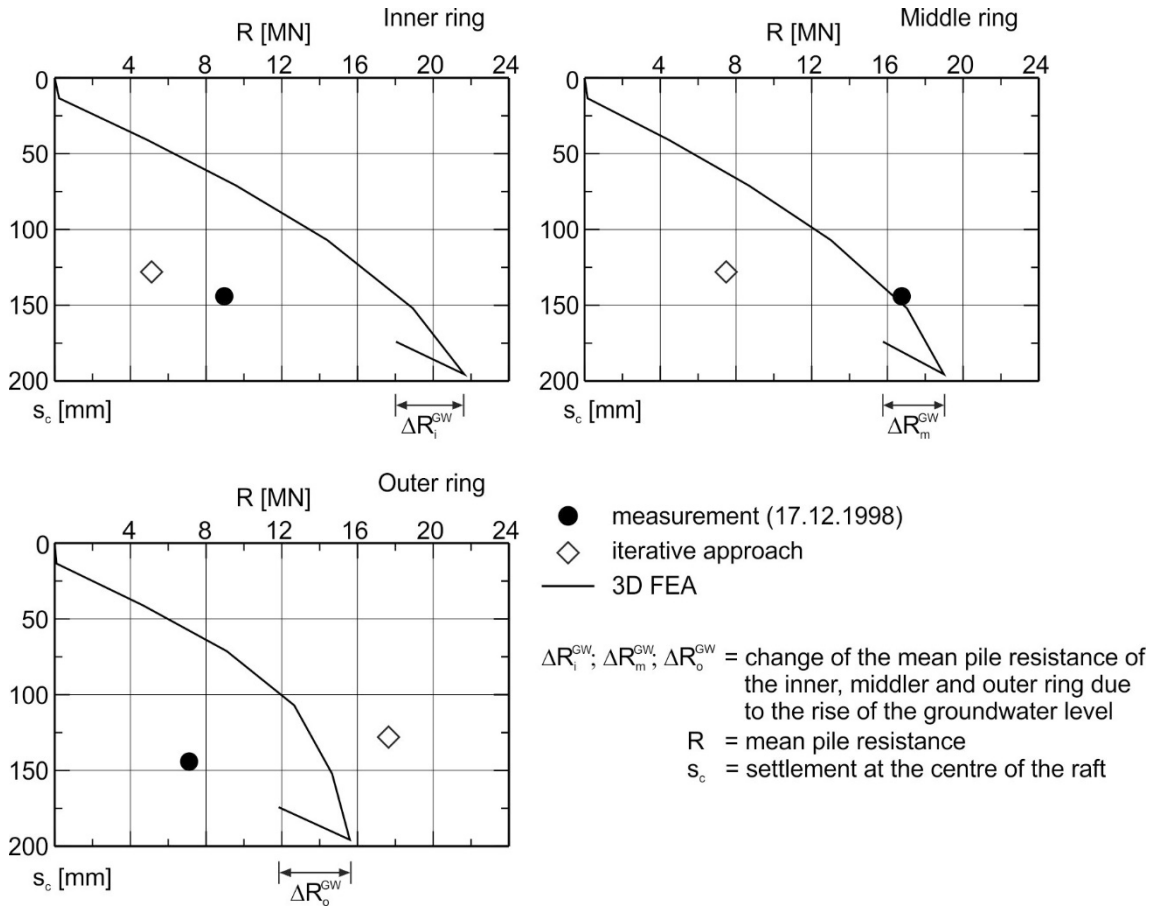


Fig. 17 Messeturm: Pile resistance

The settlement distribution along a cross section through the foundation is plotted in Fig. 16 with the measurements showing more significant differential deflection than both the 3D FEA and the iterative approach. The much stiffer raft response of the iterative approach, which gives the least differential settlement, is probably caused by the approximate modelling of the raft section where the thickness decreased gradually from 6 m to 3 m. For the iterative analysis here, this has been modeled as a constant raft thickness of 4.5 m.

The 3D FEA yields a piled raft coefficient of $\zeta_{pr} = 0.63$ (groundwater draw down) and $\zeta_{pr} = 0.60$ (natural groundwater level). Based on the assumption that the average pile load can be derived from the 12 instrumented piles, the piled raft coefficient at the time of the last documented measurement, where the ground water was situated almost at its natural level, is $\zeta_{pr} = 0.43$. With the iterative approach a piled raft coefficient of $\zeta_{pr} = 0.46$ is calculated. However, comparison of the mean pile resistances for the three different pile length, i.e. inner ring, middle ring and outer ring, show significant scatter in calculated and measured data, as shown in Fig. 17.

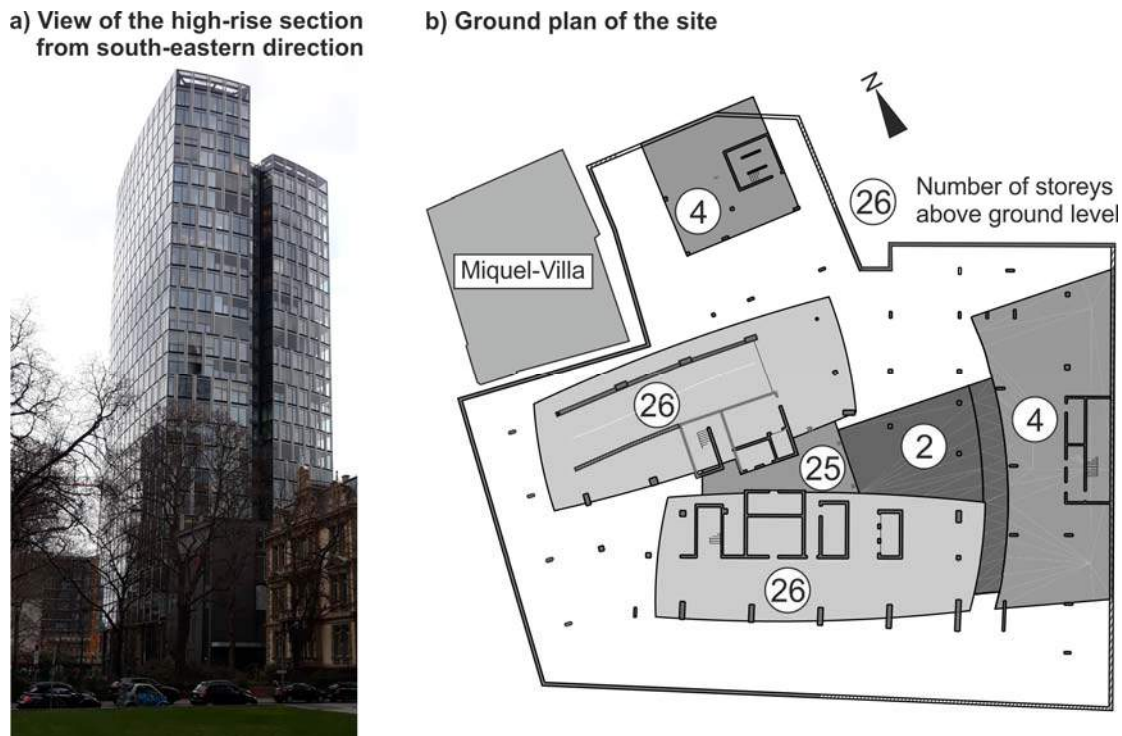


Fig. 18 WestendDuo: View of building and ground plan

4.3.2 WestendDuo (Frankfurt, Germany)

The building complex WestendDuo in Frankfurt, a reinforced-concrete skeleton construction consisting of two connected 96 m high office towers (Fig. 18a) and a low rise section with a maximum height of approximately 20 m, was constructed between November 2004 and November 2006. The WestendDuo has replaced an 83 m high office tower with a 3-storey basement. The basement area of the new building complex with a size of approximately 4100 m² is equivalent to the basement area of the demolished building. At the north-western corner of the site, the heritage-protected historic Miquel-Villa is situated in the immediate vicinity of the 4-storey basement of the WestendDuo (Fig. 18b). Loads from the WestendDuo superstructure amount to approximately

$G + Q = 695 \text{ MN} + 220 \text{ MN} = 915 \text{ MN}$ (G : dead loads; Q : live loads) and are transferred to the raft mainly in the approximately $17 \text{ m} \times 30 \text{ m}$ core area of the two towers via walls and at the edge of the building via columns (maximum column load $G + Q = 23.3 \text{ MN}$). The effective settlement inducing load (settlement inducing load minus uplift) amounts to $P_{eff} \approx 613 \text{ MN}$.

The subsoil conditions on the project site are characterized mainly by tertiary soils and rock with artificially filled soils and quaternary sand and gravel with a thickness of approximately 6 m just below the ground surface. The tertiary soils consist of Frankfurt clay with a thickness of approximately 79 m at the top underlain by the Frankfurt limestone. The natural groundwater level is situated approximately 6.8 m below the ground surface. Material parameters are summarized in Table 6.

In the course of the technical and economic design process for the foundation several design alternatives were investigated by means of three-dimensional elastoplastic finite element analysis (3D FEA) (Reul et al. 2006). A study of the cost reduction that can be achieved based on an optimized foundation design for WestendDuo was presented by Reul and Randolph (2009).

Table 7 compares the main analysis results, i.e. the maximum settlement, the deflection ratio of the raft as defined by Burland et al. (1977) and the piled raft coefficient for an unpiled raft (configuration F1) and a piled raft (configuration K3). Additionally the results of an analysis carried out with the iterative approach for configuration K3 is documented where the stiffness profile of the soil is again modelled by means of Eq. (6). The basement walls have been included explicitly in the 3D FEA model, while with the iterative approach analysis the stiffness of the raft has been increased moderately in the high-rise section to take into account the stiffness of the basement. Fig. 19 shows the layout of the foundation.

Table 6 WestendDuo: Material parameters applied in the analysis with the iterative approach.

| Analysis | Parameter | | | | |
|---------------|-----------------|--------------------------|----------|---------|--|
| PIGLET | Soil | Surface shear modulus | G_{0a} | [kPa] | $2.059 \cdot 10^4$ |
| | | Shear modulus gradient | Gm_a | [kPa/m] | $4.190 \cdot 10^2$ |
| | | Shear modulus below base | G_b | [kPa/m] | $3.600 \cdot 10^4$ |
| | Poisson's ratio | ν | [-] | 0.15 | |
| | Pile | Young's modulus | E_{pa} | [kPa] | $3.0 \cdot 10^7$ |
| Raft analysis | Soil | Young's modulus | E | [MPa/m] | Equation (6)* ¹ |
| | | Poisson's ratio | ν | [-] | 0.15 |
| | Raft | Young's modulus | E | [kPa] | $3.0 \cdot 10^7 / 9.0 \cdot 10^7$ * ² |
| | | Poisson's ratio | ν | [-] | 0.20 |

*¹ with depth of raft base below the surface of the tertiary layers $z_r = 8.7 \text{ m}$

*² increased stiffness to take into account the stiffness of basement in the high-rise section

For the unpiled raft F1 maximum settlements of $s_{max} = 137 \text{ mm}$ have been calculated. The deflection ratio $\Delta/L \approx 1/300$, where Δ is the maximum differential settlement over a length L , is critical because the resulting cracks in the concrete structure might cause problems for the impermeable basement. For the piled raft K3 the maximum settlement and the deflection ratio are significantly reduced to $s_{max} = 72 \text{ mm}$ and $\Delta/L \approx 1/500$, respectively. For configuration K3 the iterative approach yields $s_{max} = 76 \text{ mm}$ and $\Delta/L \approx 1/500$. The proportions of the load transferred to

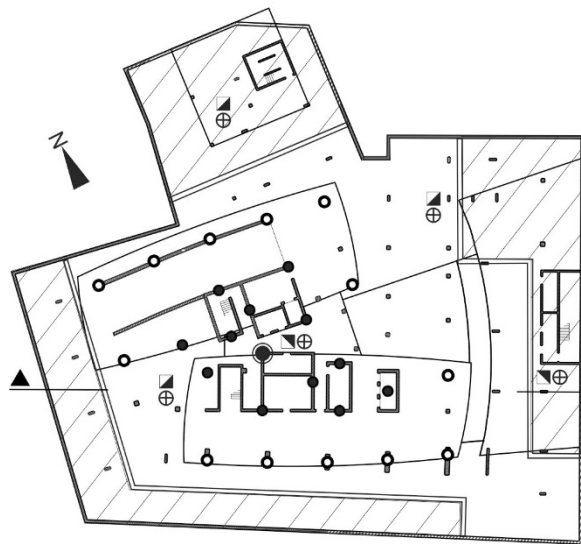
the subsoil by the piles are practically identical for the 3D FEA and the iterative approach and amount to $\zeta_{pr} = 0.380$ and $\zeta_{pr} = 0.379$, respectively.

Table 7 WestendDuo: Comparison of analysis of different foundation options

| Foundation configuration | Analysis | t_r hr / lr [m] | n [-] | L_p [m] | d_p [m] | $n \cdot L_p$ [m] | s_{max} [mm] | Δ/L [-] | ζ_{pr} [-] |
|--------------------------|--------------------|-------------------------|------------|--------------|--------------|----------------------|-------------------|-------------------|---------------------|
| F1 unpiled raft | 3D FEA | 2.4/2.4 | — | — | — | — | 137 | ~1/300 | — |
| K3 piled raft | 3D FEA | 1.8/1.2 | 26 | 25/20 | 1.2 | 585 | 72 | ~1/500 | 0.380 |
| K3 piled raft | iterative approach | 1.8*/1.2 | 26 | 25/20 | 1.2 | 585 | 76 | | 0.379 |

| | | | |
|-------|---|---------------|------------------------------|
| t_r | thickness of the raft (hr: high rise section; lr: low rise section) | L_p | pile length |
| * | increased stiffness to take into account the stiffness of basement in the high-rise section | d_p | pile diameter |
| n | number of piles | $n \cdot L_p$ | total pile length |
| | | s_{max} | maximum settlement |
| | | Δ/L | deflection ratio of the raft |
| | | ζ_{pr} | piled raft coefficient |

a) Ground plan



b) Cross section

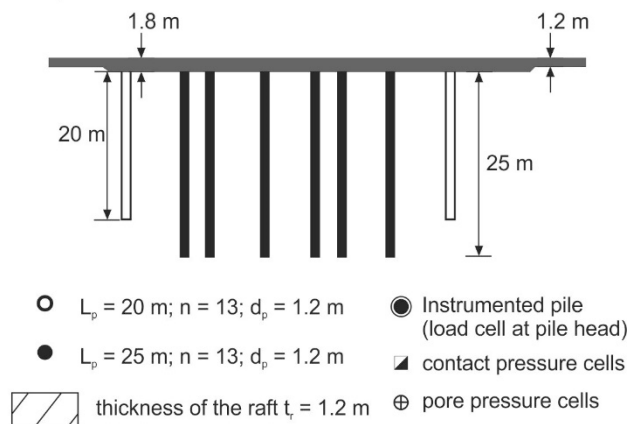


Fig. 19 WestendDuo: Layout of the foundation

Three foundation piles at WestendDuo were equipped with a load cell at the pile head, and five contact pressure cells and five pore pressure cells were placed beneath the raft to establish the load transfer to the subsoil (see plan in Fig. 19). However, during the construction process two cable connections to pile load cells were permanently damaged leaving only the measurement data of one, a 25 m long pile, available for interpretation.

The deformations of the foundation were monitored with 23 geodetic survey points located in the basement. Fig. 20 shows the maximum settlement measured in November 2006, when the building had just been finished, amounting to $s_{max} = 47$ mm. It can be concluded that even allowing for small time dependent settlements due to consolidation and creep, the maximum settlements obtained from the analyses (Table 7) will not be exceeded.

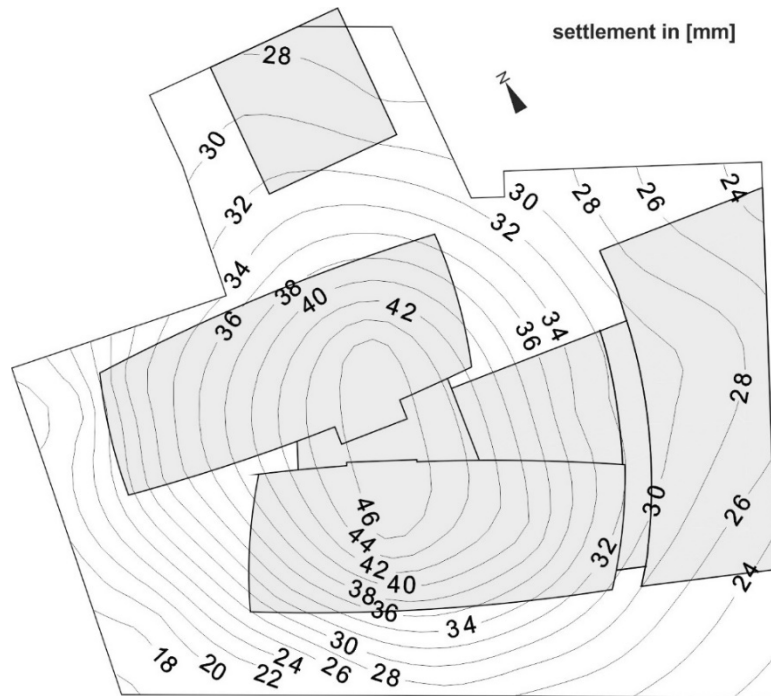


Fig. 20 WestendDuo: Measured settlements in November 2006 after the building had been finished

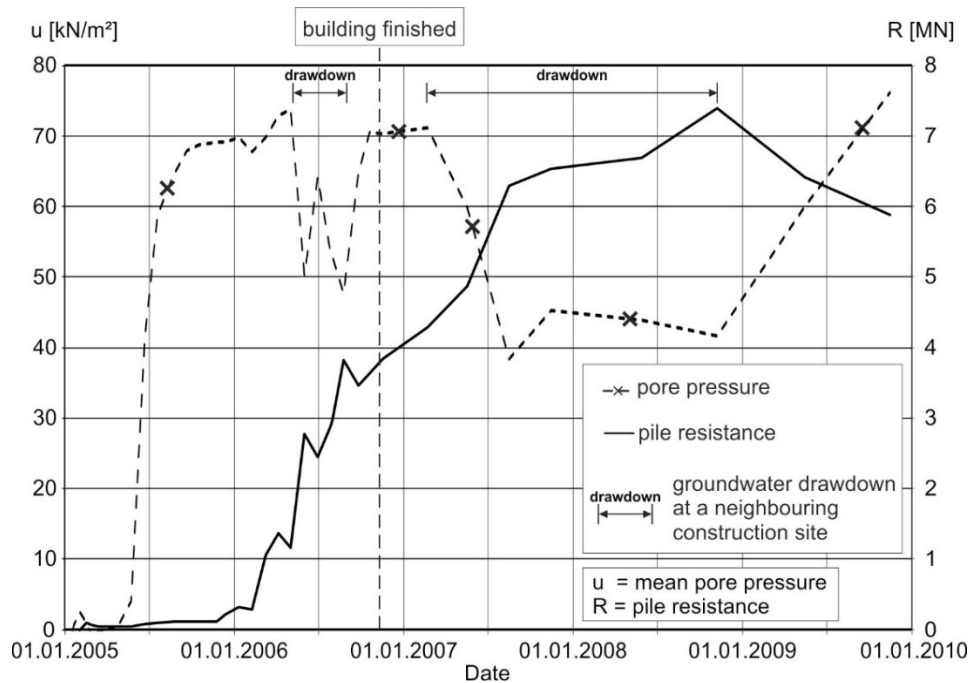


Fig. 21 WestendDuo: Measured variation of pore pressure and pile resistance with time

Fig. 21 shows the variation of the measured mean pore pressure and the measured pile resistance with time. As observed for the Messeturm the pile resistance is significantly influenced

by the groundwater level, i.e. the uplift acting on the foundation. Two groundwater drawdowns for construction sites at a distance of approximately 300 m from the WestendDuo caused a loss of uplift and therefore increase of the settlement inducing load of up to $\Delta P \approx 155$ MN. The maximum pile resistance was measured in November 2008 with $R = 7.4$ MN. The last measurement available in November 2009 showed a value of $R = 5.9$ MN. In comparison, the calculated average pile resistance amounts to $R = 8.9$ MN both for the 3D FEA and the iterative approach.

5. CONCLUSIONS

This paper has explored a range of linear and nonlinear analysis approaches for pile groups and piled rafts. These range from simple ‘lumped’ models for the entire pile group and ground-contacting pile cap (or raft), to more sophisticated tools that allow more detailed quantification of load sharing between raft and pile and among the piles within the group, and also of differential settlements across the foundation. Results from the pile group analysis, PIGLET, which has recently been enhanced to include non-linear response of individual piles, are compared with measurements from field-scale tests on small groups of piles, and also from field measurements from a large pile group. These demonstrate the beneficial effects of non-linear pile response, which helps to even out the load distribution within the group.

The finite bending stiffness of the pile cap, or the raft component for a piled raft foundation, also contributes towards evening out of the load distribution among the piles but with a penalty of increased differential settlements. In order to explore a simple approach to evaluate differential settlements and load distribution within the pile group, the paper presents an iterative approach that allows the analysis of piled rafts by means of two complementary analyses for a pile group and a raft. This approach is illustrated by comparing results with (a) those from 3D finite element analysis of a hypothetical piled raft with relatively few, widely spaced, piles; and (b) in relation to field measurements from instrumented case histories of piled rafts.

REFERENCES

- Abdelrazaq, A., Badelow, F., SungHo-Kim and Poulos, H.G., 2011. Foundation design of the 151 story Incheon Tower in a reclamation area. *Geotechnical Engineering Journal of the SEAGS & AGSSEA* Vol. 42 No.2, pp 85–93.
- Basile, F., 2003. Analysis and design of pile groups. *Numerical Analysis and Modelling in Geomechanics* (ed. J. W. Bull), Spon Press (Taylor & Francis Group Ltd), Oxford, Chapter 10, 278-315.
- Basile, F., 2013. A practical method for the non-linear analysis of piled rafts. *Proc. 18th Int. Conf. on Soil Mechanics and Foundation Engineering*, Paris, 4pp.
- Burland, J.B., Broms, B.B. and De Mello, V.F.B., 1977. Behaviour of foundations and structures. *Proc. 9th Int. Conf. Soil Mech. Found. Engng*, Tokyo 2, pp 495–546.
- Butler, F.G., 1975. Heavily over-consolidated clays - Review paper: Session III. *Proc. Conf. Settlements of Structures*, Cambridge, pp 531-578.
- Butterfield, R. and Banerjee, P. K., 1971. The elastic analysis of compressible piles and pile groups. *Géotechnique* 21(1), 43-60.
- Caputo, V. and Viggiani, C., 1984. Pile foundation analysis: a simple approach to non linearity effects. *Rivista Italiana di Geotecnica*, 18 (2), 32-51.
- Clancy, P. and Randolph, M.F., 1993. An approximate analysis procedure for piled raft foundations. *Int J. Num. and Anal. Methods in Geomechanics*, 17(12), 849-869.

- Coffey, 2007. CLAP (Combined Load Analysis of Piles) – Users’ Manual. Coffey Geotechnics, Sydney, Australia.
- Doherty, J.P., 2018. LAP – software for lateral pile analysis. www.geocalcs.com/LAP.
- Ensoft, 2016. GROUP –software for pile group analysis. Ensoft Inc., Austin, USA.
- Ensoft, 2016. LPILE –software for lateral pile analysis. Ensoft Inc., Austin, USA.
- Geocentrix, 2017. Repute 2.5: Onshore pile design and analysis. Users’ manual. Geocentrix Ltd.
- Goosens, D. and Van Impe, W.F., 1991. Long term settlements of a pile group in sand overlaying a clay layer. Proc. 10th European Conf. on Soil Mechanics and Foundation Engineering, Florence, Vol. 1, pp 425-428.
- Katzenbach, R., Arslan, U. & Moormann, C., 2000. Piled raft foundation projects in Germany. In Design Applications of Raft Foundations, pp. 323–391. Thomas Telford, London.
- Mandolini, A., Di Laora, R. and Iodice, C., 2017. Simple approach to static and seismic design of piled rafts. Proc. 3rd Bolivian Int. Conf. on Deep Foundations, Vol. 1, pp 107-124.
- McCabe, B.A. and Lehane, B.M., 2006. Behavior of axially loaded pile groups driven in clayey silt. J. of Geotechnical and GeoEnvironmental Engineering, ASCE 132(3), 401-410.
- Mindlin, R. D. (1936). Force at a point in the interior of a semi-infinite solid. Physics 7, 195-202.
- O’Neill, M.W., Hawkins, R.A. and Mahar, L.J., 1980. Field Study of Pile Group Action; Final Report. Report FHWA RD-81-002, Federal Highway Administration, U.S. Dept of Transportation.
- O’Neill, M.W., Hawkins, R.A. and Mahar, L.J., 1982. Load transfer mechanisms in piles and pile groups. J. of the Geotechnical Engineering Div., ASCE, Vol. 108(GT12), 1605-1623.
- Pirrello, S. and Poulos, H.G., 2014. Comparison of four pile group analysis programs. Advances in Foundation Engineering, Eds K.K. Phoon, T.S. Chua, H.B. Yang and W.M. Cham, Research Publishing Services. ISBN: 978-981-07-4623-0.
- Poulos, H.G., 1968. Analysis of the settlement of pile groups. Géotechnique 18(4), 449-471.
- Poulos, H.G., 1979. Settlement of single piles in non- homogeneous soil. J. Geotech. Engng, ASCE, 105(GT5), 627-641.
- Poulos, H.G., 1989. Pile behaviour - theory and application. 29th Rankine Lecture, Géotechnique 39(3) 365-415.
- Poulos, H.G., 1990. DEFPIG Users’ Manual. Center for Geotechnical Research, University of Sydney, Australia.
- Poulos, H.G., 1994. An approximate numerical analysis of pile-raft interaction. Int. J. of Numerical and Analytical Methods in Geomechanics, 18, 73-92.
- Poulos, H.G., 2001. Piled raft foundations: design and applications. Géotechnique 51(2), 95-113.
- Poulos, H.G., Small, J.C. and Chow, H., 2011. Piled raft foundations for tall buildings, Geotechnical Engineering Journal of the SEAGS & AGSSEA Vol. 42 No.2 pp 78–84.
- Randolph M.F., 1981. The response of flexible piles to lateral loading. Géotechnique, Vol 31, No 2, pp 247-259.
- Randolph M.F., 1983. Design of piled raft foundations. Proc. Int. Symp. on Recent Developments in Laboratory and Field Tests and Analysis of Geotechnical Problems, Bangkok, pp 525-537.
- Randolph M.F., 1994. Design methods for pile groups and piled rafts. Proc. 13th Int. Conf. on Soil Mech. and Found. Eng., New Delhi, Vol. 5, pp 61-82.
- Randolph, M. F., 2003. PIGLET: Analysis and design of pile groups. Users’ Manual, Version 4-2, Perth.
- Randolph, M.F., 2003. RATZ: Load transfer analysis of axially loaded piles. Users’ Manual, Version 4-2, Perth.

- Randolph, M. F., 2019. PIGLET: Analysis and design of pile groups. Users' Manual, Version 6-1, Perth.
- Randolph M.F. and Wroth C.P., 1978. Analysis of deformation of vertically loaded piles. *J. of the Geot. Eng. Div., ASCE*, Vol 104, No GT12, pp 1465-1488.
- Reul, O., 2000. In-situ measurements and numerical studies on the bearing behaviour of piled rafts. PhD Thesis, Darmstadt University of Technology, Darmstadt, Germany (in German).
- Reul, O., 2004. Numerical study of the bearing behaviour of piled rafts. *International Journal of Geomechanics*, 4(2), 59-68.
- Reul, O., Ehrhardt, G. and Rummel, B., 2006. Entwurfsoptimierung einer Hochhausgründung im Frankfurter Ton. *Vorträge des 5. Kolloquiums Bauen in Boden und Fels; Technische Akademie Esslingen*, pp 309-318.
- Reul, O. and Randolph, M.F., 2003. Piled rafts in overconsolidated clay – Comparison of in-situ measurements and numerical analyses. *Géotechnique*, 53(3), 301-315.
- Reul, O. and Randolph, M.F., 2004. Design strategies for piled rafts subjected to non-uniform vertical loading. *J. Geotech. and Geoenv. Eng. Div, ASCE*, 130(1), 1-13.
- Reul, O. and Randolph, M.F., 2009. Optimised Design of Combined Pile Raft Foundations. *Proc. International Conference on Deep Foundations – CPRF and Energy Piles, 15 May 2009, Frankfurt am Main, Darmstadt Geotechnics No. 18*, 149-169.
- Rollins, K.M., Olsen, K.G., Jensen, D.H., Garrett, B.H., Olsen, R.J. and Egbert, J.J., 2006. Pile spacing effects on lateral pile group behaviour: Analysis. *J. Geotech. and Geoenv. Eng. Div, ASCE*, 132(10), 1272-1283.
- Rollins, K.M., Peterson, K.T. and Weaver, T.J., 1998. Lateral load behaviour of full-scale pile group in clay. *J. Geotech. and Geoenv. Eng. Div, ASCE*, 124(6), 468-478.
- Russo, G., 1998. Numerical analysis of piled rafts. *Int. J. of Numerical and Analytical Methods in Geomechanics*, 22, 477-493.
- Russo, G., Abagnara, V., Poulos, H.G. and Small, J.C., 2012. Re-assessment of foundation settlements for the Burj Khalifa, Dubai. *Acta Geotechnica*, DOI 10.1007/s11440-012-0193- .
- Sheil, B.B., McCabe, B.A., Comodromos, E.M. and Lehane, B.M., 2018. Pile groups under axial loading: an appraisal of simplified non-linear prediction models. *Géotechnique*, <https://doi.org/10.1680/jgeot.17.R.040>.
- Small, J.C. and Poulos, H.G., 2007. A method of analysis of piled rafts. *Proc 10th ANZ Conf. on Soil Mechanics and Geotechnical Engineering, Vol. 1*, pp 550-555.
- Small, J.C. and Zhang, H.H., 2002. Behaviour of piled raft foundations under lateral and vertical loading. *International Journal of Geomechanics* 2(1), 29-45.
- Sommer, H., Tamaro, G. and DeBenedictis, C., 1991. Messe Turm, foundations for the tallest building in Europe. *Proc. 4th International Conference on Piling and Deep Foundations, Balkema, Rotterdam*, pp 139-145.
- Tochnog, 2019. TOCHNOG Professional – Finite Element Analysis. Tochnog Professional Company, Nijmegen, The Netherlands.